Fermi National Accelerator Laboratory

FERMILAB-Conf-90/138-E
[E-741/CDF]

Top Quark and SUSY Searches at CDF *

The CDF Collaboration

presented by

G. P. Yeh
Fermi National Accelerator Laboratory
P.O. Box 500
Batavia, Illinois 60510

May 17, 1990

* To be published in the proceedings of the Les Rencontres de Physique de la Vallee D'Aosta, LaThuile, Italy, March 18-24, 1990.

CDF/PUB/HEAVYFLAVOR/PUBLIC/1164

Top Quark and SUSY Searches at CDF

CDF Collaboration

Presented by
G. P. Yeh
Fermi National Accelerator Laboratory

Abstract

Searches for the top quark in $p\bar{p}$ collisions at $\sqrt{s} = 1.8$ TeV are described. The analyses are based on data with an integrated luminosity of 4.4 pb^{-1} recorded with the Collider Detector at Fermilab in the 1988-1989 run. An upper limit on the $t\bar{t}$ cross section is obtained. The top quark with mass below 89 GeV/c^2 is excluded at the 95% CL. Prospects for searches for the top quark in the future are presented.

We also briefly present results on searches for supersymmetric particles.

Pub. Proceedings Les Rencontres de Physique de la Vallee D'Aosta, LaThuile, Italy, March 18-24, 1990.

1 Introduction

The '88 – '89 Run was a wonderful success for the Tevatron and for the Collider Detector at Fermilab [1] , thanks to the hard work over many years by everyone involved. The Tevatron performed well beyond expectations. Since the middle of the run, CDF has presented/published results on top quark searches [2,3], Z [4], W [5], b-quark, charm-quark, QCD and photon physics. Some of the recent results have been presented by 4 speakers [6] , at this Conference. In this talk, we present new results on recent searches for the top quark and for supersymmetric (SUSY) particles.

A large number of collisions is necessary to produce the massive top quark, thus requiring high integrated beam luminosity. The goal for the integrated luminosity recorded on tape had been 1 pb^{-1}, Fermilab promised 1 pb^{-1} and delivered 9.7 pb^{-1}. The data sample recorded on tape by CDF corresponded to 4.7 pb^{-1} , which was 200 times the sample from the previous run in 1987.

Results from both the $e\,\mu$ and the $e + jets$ top search analyses were first presented at the 1989 winter conferences [7] , based on the 2 pb^{-1} of data recorded up to February 1989. By the end of the run in May, with 4.4 pb^{-1} of data, the $e\,\mu$ analysis obtained the result $M_{top} > 72$ GeV/c^2 at 95% CL, while the $e+jets$ analysis obtained $M_{top} > 77$ GeV/c^2. These results have been published. [2,3,5] .

Heavy top quarks produced in $p\bar{p}$ collisions at $\sqrt{s} = 1.8$ TeV have numerous distinctive signatures. With good identification and resolution for electrons, muons, jets, and neutrinos (via missing transverse energy $\not\!\!E_T$), CDF can search for the top quark in many channels. The efficiencyiy of each channel to detect the top quark varies as a function of M_{top} . As we probe higher M_{top} regions, different channels become more effective.

Since September, we have explored other channels. We discuss signals for the top quark in the next section, and briefly review the previous results in Section 3. Preliminary results with the new channels are presented in Sections 4 and 5. We also update b-quark and J/ψ results in Section 6, and searches for SUSY particles in Section 7.

2 Signals for the Top Quark

2.1 t Production Cross-Sections

The top quark production cross sections [8,9] via the reactions (1) $p\bar{p} \rightarrow t\bar{t} + X$ and (2) $p\bar{p} \rightarrow W + X; W \rightarrow t\bar{b}$ are shown in Figure 1 for $\sqrt{s} = 1.8$ TeV (Fermilab Tevatron Collider) and for $\sqrt{s} = 0.63$ TeV ($S\bar{p}pS$ Collider) . With two top quarks in each event, the signatures of $t\bar{t}$ are more distinctive than those of $t\bar{b}$ from W decay. If M_{top} is between 40 GeV/c^2 and M_W, $W \rightarrow t\bar{b}$ has higher cross-section than $t\bar{t}$ at $\sqrt{s} = 0.63$ TeV. Between the energies of the two colliders, the $t\bar{t}$ production cross section increases by a factor of 25 for a top mass of 80 GeV, and by larger factors for higher top masses.

At $\sqrt{s} = 1.8$ TeV, $t\bar{t}$ pair production is the dominant process for producing top quarks. The uncertainties in the predicted cross-sections are estimated to be about 30%. In the mass region near $M_{top} \approx 80$ GeV/c^2 , $\sigma_{t\bar{t}}(M_{top}) \approx 40\ \sigma_{t\bar{t}}(2M_{top})$, and variation in cross-section by a factor of 2 corresponds to about 10 GeV/c^2 change in top mass . In the absence of discovery of the top quark, the experiment measures the upper limit on the production cross-section, which is compared with the theoretical prediction to obtain a limit on the top quark mass. Both the mass and the production cross-section will be measured when the top quark is discovered . In the '88 – '89 data sample of 4.4 pb^{-1}, 1200 (30) events are expected to have been produced in CDF if $M_{top} = 80$ (160) GeV/c^2 .

2.2 t Decay Channels

In the standard model, the t quark is expected to decay to the lighter b quark and a W boson. In this charged current decay, the W boson may be either real or virtual depending on the mass of the decaying t quark. Thus, each $t\bar{t}$ pair will decay into $W^+bW^-\bar{b}$. With two W bosons and two b-quarks in each event, $t\bar{t}$ events provide many signals for detection. Each W subsequently decays into two light quarks (hadronic decay, with a branching fraction of 2/3) or two leptons (charged lepton + neutrino, with a branching fraction of 1/9 for each of e, μ, and τ). The $t\bar{t}$ pair therefore decays via hadron-hadron (multi-jets), lepton-hadron ($e + jets, \mu + jets, \tau + jets$), or

lepton-lepton ($ee, \mu\mu, \tau\tau, e\mu, e\tau, \mu\tau$) modes .

The multi-jet signal of the hadron-hadron mode with a branching fraction of 4/9 is difficult to observe due to background from QCD jets which is orders of magnitude higher. In the lepton-hadron mode, the high P_T charged lepton + neutrino + jets signature reduces the QCD, $b\bar{b}$, and $gb\bar{b}$ backgrounds effectively; the remaining large background is from $p\bar{p} \rightarrow W+$ multi-jets. Identification of at least one of the b and $\bar{b}$ in the decay of the $t\bar{t}$ pair will be the key to separating top quark candidates from the $W+$ multi-jets background.

The di-lepton mode, especially the $e\mu$ decay mode, with clean signal to background, provides the most unambiguous $t\bar{t}$ signatures. For the eμ final state with a high P_T electron and a high P_T muon, the backgrounds are small and are from the decays of $b\bar{b}$, $gb\bar{b}$, and $Z \rightarrow \tau\tau; \tau \rightarrow$ e or μ. The $t\bar{t}$ signal can be separated easily from background since both leptons are isolated and have eμ opening angle distribution which is relatively flat. Leptons from $gb\bar{b}$ or $b\bar{b}$ are not isolated. For the $b\bar{b}$ and $Z \rightarrow \tau\tau$ backgrounds, the leptons are predominantly back-to-back while the opening angle between the leptons is small for $gb\bar{b}$. Other di-lepton final states such as ee and $\mu\mu$ have large additional Z and Drell-Yan backgrounds which have characteristics (such as missing transverse energy, di-lepton invariant mass and opening angle) that are distinguishable from the top signal.

3 Previous Results

The best e^+e^- results from LEP and recent results from UA1 and UA2 on searches for the top quark have been reported at this Conference by speakers from each of the experiments. Here we summarize previous CDF results that have been published.

The $e + jets$ analysis [3] searched for $p\bar{p} \rightarrow t\bar{t} \rightarrow W^+b\,W^-\bar{b} \rightarrow e\nu b\,q_1q_2\bar{b}$ events. The two light quarks (q_1 and q_2) from the decay of a W subsequently fragment into two observable jets. For $M_{top} < 100$ GeV/c^2 , the b and $\bar{b}$ quarks have soft P_T spectra and are difficult to observe. The search was based on the transverse mass $M_T^{e\nu}$ distribution [10] of the electron and the neutrino ($\not\!\!E_T$) in events with a high E_T electron and two or more jets. The background to this signal is $W + jets$ in

which the W also decays into an electron and a neutrino. For M_{top} below M_W, the W in the decay of the top quark is virtual, thus $M_T^{e\nu}$ for the top quark should be less than $M_T^{e\nu}$ for a real W. For M_{top} above M_W, the W in the decay of the top quark is real, thus the shape of $M_T^{e\nu}$ for the top signal is similar to the shape for $W + jets$ background. Distinguishing top quark from $W + jets$ using transverse mass distribution is valid only for M_{top} below M_W. The $e + jets$ analysis excluded the region 40 GeV/c^2 $< M_{top} <$ 77 GeV/c^2 at 95% CL.

The $e\,\mu$ analysis [2] searched for $p\bar{p} \rightarrow t\bar{t} \rightarrow W^+b\,W^-\bar{b} \rightarrow e\nu b\,\mu\nu\bar{b}$ events. The signal for $t\bar{t}$ is a high P_T electron and an oppositely charged high P_T muon. The data sample contains one event in the top quark signal region. This event has an isolated electron with $E_T(e)$ of 31.7 GeV and an isolated opposite sign muon with $P_T(\mu)$ of 42.5 GeV/c with a di-lepton azimuthal opening angle of 137 degrees. Other characteristics of the event include the presence of a second muon candidate with a transverse momentum of 10 GeV/c in the forward muon detector, and a jet with calorimeter transverse energy deposition of 14 GeV. A firm conclusion about the identity of this event is not possible. Given that one event exists in the signal region, an upper limit on the $t\bar{t}$ cross-section can be calculated and compared with the cross-section predicted as a function of M_{top}. The $e\mu$ analysis excluded the region 28 GeV/c^2 $< M_{top} <$ 72 GeV/c^2 at 95% CL.

A third analysis [5] which is independent of top decay modes measured the ratio $\sigma(W \rightarrow e\nu)/\sigma(Z \rightarrow ee)$ and concluded $M_{top} > 35$ GeV/c^2. Thus these 3 CDF results compliment each other and set a lower limit of 77 GeV/c^2 on the mass of the top quark.

Preliminary results have been obtained from new top quark searches in the last few months. The efficiency (after the branching ratio of 2/81) for detecting $t\bar{t} \rightarrow e\nu b\,\mu\nu\bar{b}$ increases as a function of M_{top} and has been determined in the $e\mu$ analysis to be 12%, 17%, and 20% at M_{top} = 70, 80, and 90 GeV/c^2, respectively. Thus, the $e\mu$ analysis has an efficiency of 0.5% for detecting $t\bar{t}$ pairs produced in CDF, for $M_{top} = 90$ GeV/c^2. There are many ways to improve this efficiency, such as relaxing the lepton selection, extending the search from the 'Central' detector region to smaller angle ('Forward' and 'Backward') regions, and searching in more $t\bar{t}$ decay channels.

The detection efficiency of the τ lepton in $t\bar{t}$ decays increases with M_{top}. Top quark decays containing the τ lepton have been included in the analyses if the subsequent decay of the τ produces an electron or a muon. The identification of taus can increase the efficiency for finding $t\bar{t}$ in the future.

Results and experience from the $e\mu$ analysis have been applied to a combined $e\mu$, ee, or $\mu\mu$ di-lepton search which is presented in Section 4. The identification of b-quarks in high P_T lepton $+jets$ events also constitutes a clean signal for $t\bar{t}$ production. Preliminary results from such a *b-tagging* search will be presented in Section 5.

4 di-lepton Search

In this Section, we present results on a search for $t\bar{t}$ pairs decaying into final states containing $e\mu$, ee, *or* $\mu\mu$ di-leptons. Understanding of the central electron and central muon and of the top signal vs the $b\bar{b}$ background obtained in the $e\mu$ analysis are immediately applicable. By searching for di-leptons instead of requiring an e and a μ in each event, the $e\mu$, ee or $\mu\mu$ channels are combined directly to provide better acceptance for $t\bar{t}$ events.

The $e\mu$ channel was analyzed first for two reasons. The ee and the $\mu\mu$ channels together have the same branching ratio as the $e\mu$ channel. In the $e\mu$ analysis, by requiring leptons from different families, lepton pair backgrounds from Drell-Yan and Z^0 production are eliminated. In the ee and $\mu\mu$ analyses, these backgrounds are removed based on kinematic quantities that are characteristic of the Drell-Yan and Z^0 events. The distributions of the di-lepton invariant mass, the missing transverse energy of the event, and the di-lepton azimuthal angular separation for the $t\bar{t}$ signals are particularly distinguishable from those of the Drell-Yan and Z^0 events.

4.1 Trigger

Detailed descripton of the CDF detector has been published [1] . An inclusive electron trigger collected the $e\mu$ and ee events. The efficiency of this trigger has been studied using data taken at lower trigger thresholds and using W and Z events from

an independent trigger. We find that this trigger is 98.0 $\pm$ 0.5% efficient for single electron with $E_T(e) > 15$ GeV. An inclusive muon trigger collected events for the $\mu\mu$ channel. Preliminary results show that this trigger is 90% efficient for single muon with $P_T(\mu) > 15$ GeV/c.

4.2 Central Electron Selection

We have tight electron cuts and loose electron selection cuts. For $e\mu$ the electron is required to pass tight cuts. For ee one electron must pass the tight cuts and the other the loose cuts. To pass the tight cuts, electron candidates must be inside the region $|\eta| < 1.0$ and must satisfy the following. (1) A calorimeter cluster must have $E_T(e) > 15$ GeV, a ratio of hadronic energy to EM energy of less than 0.05, and a lateral shape consistent with that of an electron shower. Fiducial cuts to avoid cracks between calorimeter modules are applied. (2) The ratio of the cluster energy to track momentum must be less than 1.5. (3) A strip chamber cluster must have energy profiles in both the ϕ (azimuth) and z (along the beam direction) views consistent with an electron shower. (4) The distance between the strip chamber shower position and the extrapolated track position must be less than 1.5 cm in the ϕ direction and less than 3.0 cm in the z direction.

The electron fiducial volume covers 84% of the solid angle in the region $|\eta| <$ 1.0. For electrons inside the fiducial volume with $E_T(e) > 20$ GeV, the efficiency of the electron selection as measured using a sample of $Z^0 \rightarrow e^+e^-$ is 0.77 $\pm$ 0.03 and is consistent with test beam measurements.

Electron candidates without a matching VTPC track or with a second nearby oppositely charged CTC track forming a low e^+e^- effective mass are rejected as photon conversion candidates. The low-mass pair cut also rejects electrons from Dalitz decays of neutral pions. The photon conversion cuts cause an inefficiency of 5% for identifying electrons.

The loose cuts for the second electron for ee events are : (1) The transverse energy in the towers within a cone of R $\equiv \sqrt{(\Delta\phi)^2 + (\Delta\eta)^2} = 0.4$, excluding the electron energy, is less than 5 GeV. (2) A calorimeter cluster must have a ratio of hadronic energy to EM energy of less than 0.125. and (3) Standard Fiducial cuts .

The loose cuts are $\gtrsim$ 99% efficient for electrons inside the fiducial volume.

4.3 Central Muon Selection

Muon candidates are selected inside the region $|\eta| < 1.2$ and must satisfy the following. (1) A minimum ionization requirement is imposed. The calorimeter tower to which the CTC track points is required to contain less than 2 GeV of energy in the EM compartment, less than 6 GeV of energy in the hadronic compartment, but more than 0.1 GeV in the sum of the two compartments. (A minimum ionizing particle will deposit on the average 0.3 GeV and 2 GeV of EM and hadronic energy respectively). Fiducial cuts are applied to avoid cracks between calorimeter modules. (2) A P_T threshold requirement is imposed. For candidates with an associated track in the muon chambers, $P_T(\mu)$ must be greater than 5 GeV/c and the azimuthal separation between the extrapolated CTC track and the muon chamber track must be less than 10 cm. In addition, candidates with $P_T(\mu) > 10$ GeV/c having no associated muon chamber track are accepted if the transverse energy in the towers within a cone of R = 0.4, excluding the muon energy, is less than 5 GeV. This extends muon detection out to $|\eta| < 1.2$.

The muon fiducial volume covers 85% of the solid angle in the region $|\eta| < 1.2$. For muons inside the fiducial volume with $P_T(\mu) > 20$ GeV/c, the efficiency of the muon selection as measured using a sample of $Z^0 \rightarrow \mu^+\mu^-$ is 0.98 $\pm$ 0.02 and 0.96 $\pm$ 0.02 for muons with and without a muon chamber segment, respectively.

4.4 Z removal for the ee, $\mu\mu$ channels

We defined a top quark signal region with $E_T(e) > 15$ GeV and $P_T(\mu) > 15$ GeV/c for the $e\mu$ channel. This requirement minimizes $b\bar{b}$ and $gb\bar{b}$ backgrounds. We also require $E_T(e) > 15$ GeV and $P_T(\mu) > 15$ GeV/c for the ee and the $\mu\mu$ channels, respectively. As we look in more channels and/or at more data, some $b\bar{b}$ and $gb\bar{b}$ decaying into di-lepton events may be found in the signal region. For the $b\bar{b}$ background, the leptons are predominantly back-to-back while the opening angle between the leptons is small for $gb\bar{b}$. There are many ways to remove these and the larger Z and Drell-Yan backgrounds. We make the following additional requirements:

- the invariant mass $M_{l^+l^-}$ is not in the mass window 75 to 105 GeV/c^2.
- missing transverse energy $\not\!\!E_T \geq$ 20 GeV.
- $20^o \leq \Delta\phi_{l^+l^-} \leq 160^o$ for the azimuthal angular separation.

The distribution of the ee invariant mass, M_{ee}, $\not\!\!E_T$, and $\Delta\phi_{ee}$ for the $t\bar{t}$ are distinct from the backgrounds and are shown in Figure 2, Figure 3, and Figure 4, respectively. Figure 5 shows the plot of $\Delta\phi_{ee}$ vs. $\not\!\!E_T$ after the M_{ee} window cut. Figure 6 shows the plot of $\Delta\phi_{\mu\mu}$ vs. $\not\!\!E_T$ after the $M_{\mu\mu}$ window cut. In each of Figures 2 to 6, there are 4 plots for the $t\bar{t}(M_{top} = 80)$, $t\bar{t}(M_{top} = 90)$, Z Monte Carlo samples and for the data. For the histograms, the plots for the $t\bar{t}$ samples have been normalized to 4.4 pb^{-1}, from the generated samples of 268 pb^{-1} and 732 pb^{-1}. As shown in the talk, the six low $\Delta\phi_{\mu\mu}$ events are non-isolated punch-through particles with back-to-back jets. We have required lepton isolation in the calorimetry and should also require isolation in the tracking chamber for muons. No ee or $\mu\mu$ events pass the above kinematic cuts.

For $t\bar{t}(M_{top} = 80)$, we expect 4.6 + 1.4 + 1.5 $e\mu$, ee, $\mu\mu$ events, respectively, taking into account muon trigger efficiency. Similarly for $t\bar{t}(M_{top} = 90)$, we expect 3.0 + 0.7 + 1.0 events. The top quark detection efficiency for ee and $\mu\mu$ channels combined is $\approx$ 60 % of the efficiency of the $e\mu$ channel at M_{top} between 80 and 90 GeV/c^2. The $t\bar{t}$ detection efficiency for the $e\mu$ channel was determined previously to be 12%, 17%, and 20% at M_{top} = 70, 80, and 90 GeV/c^2 , respectively. Thus, we expect the upper limit on the $t\bar{t}$ production cross-section to be reduced by a factor of $\gtrapprox$ 2 and the limit on the top mass to be increased by $\gtrapprox$ 10 GeV/c^2.

4.5 Top quark mass limit

Given one event in the signal kinematic region, an upper limit on the $t\bar{t}$ cross section is obtained as a function of M_{top} as in the $e\mu$ analysis. This upper limit cross section takes into account several sources of systematic uncertainty, including uncertainties in lepton identification efficiencies, the t quark P_T distribution, t quark fragmentation and integrated luminosity. These uncertainties have been studied in detail for the $e\mu$ analysis.

The systematic uncertainties are added in quadrature. The total uncertainty is used as the standard deviation of a Gaussian distribution which is convoluted with the Poisson statistical probability. The resulting distribution is used to obtain the 95% CL upper limit on the number of events in the signal region as a function of M_{top}. This number is used along with the Monte Carlo calculation of $t\bar{t}$ detection efficiency as a function of M_{top} , the integrated luminosity and the semi-leptonic branching ratio to provide an upper limit on the $t\bar{t}$ production cross section.

The relatively large luminosity uncertainty has been determined with higher precision to be smaller and will soon be finalized. The overall uncertainty in acceptance for the dilepton analysis has been estimated to be 20%, which is comparable to the uncertainty in $e\mu$ analysis. The cross-section and mass limits are not sensitive to small changes in the uncertainty.

The new upper limit cross-section from the di-lepton analysis is shown in Figure 7, together with a theoretical calculation of the $t\bar{t}$ production cross section [8,9] and the upper limit cross-section from the $e\mu$ analysis. The 95% CL upper limit cross section curve intersects the lower edge of the theoretical calculation band at $M_{top} = 84$ GeV/c^2.

5 lepton $+$ *jets* $+$ soft muon *b-tagging*

The $e + jets$ analysis [3] searched for $p\bar{p} \rightarrow t\bar{t} \rightarrow W^+b\,W^-\bar{b} \rightarrow e\nu b\,q_1q_2\bar{b}$ events, as described in Section 3. A $\mu + jets$ analysis has searched similarly for $t\bar{t} \rightarrow W^+bW^-\bar{b} \rightarrow \mu\nu bq_1q_2\bar{b}$ events. The distributions in lepton P_T , jet-multiplicity, and transverse mass of the lepton and the neutrino are in excellent agreement between the $\mu + jets$ and the $e + jets$ data.

One or both of the b and $\bar{b}$ in these decays of $t\bar{t}$ pairs can decay into $\mu + \nu + c$. (The sequential decay of a c-quark may also contain a muon.) Thus the detection of a low P_T muon can provide a tag for the b . The main background in our lepton $+$ $jets$ events are from $p\bar{p} \rightarrow W + jets$. The existence of b-quarks in high P_T lepton $+$ large $\not\!\!E_T$+$jets$ data would distinguish the $t\bar{t}$ events from the $W + jets$ background and provides a clean signal for top quark production.

For the *b-tagging* , the soft muon must satisfy the following. A candidate must have an associated track in the muon chambers. $P_T(\mu)$ must be less than 15 GeV/c and the azimuthal separation between the extrapolated CTC track and the muon chamber track must be less than 15 cm. The separation R between the muon and the two highest E_T jets must be greater than 0.5.

The efficiency of the lepton + *jets* + soft muon *b-tagging* analysis for detecting $t\bar{t}$ is 0.18%, at $M_{top} = 80$, and 0.23%, for M_{top} from 85 to 90 GeV/c^2 . While the efficiency is presently only $\approx$ 30% of the efficiency of the di-lepton channel, it will be increased by several factors in the future : (1) for the higher mass top quark that will be searched with more data, the *b*-quark and the soft muon will have higher P_T and will be observed more efficiently (2) since the soft lepton will have higher P_T, it will be possible to search also for soft electrons (3) the η coverage of the muon chambers will be extended, thus providing better acceptance. In addition to *b-tagging* using soft leptons, we will also have the Silicon Vertex Detector to observe the *b*-quarks in the next run.

Since $t\bar{t}$ candidates from this analysis would not overlap with candidates from the di-lepton analysis, we can add the two sensitivities together, resulting in a more stringent limit on $t\bar{t}$ production cross-section which is also shown in Figure 7. The 95% CL upper limit cross-section curve intersects the lower edge of the theoretical calculation band at $M_{top} = 89$ GeV/c^2.

6 Results on b and c quarks

There are several CDF analyses related to b and c quarks . We would like to simply show preliminary results on :

(1) detecting B mesons (Figure 8a) via the decay $B \rightarrow e+D^0+X$; $D^0 \rightarrow K\pi$

(2) $b\bar{b}$ bound state $\Upsilon \rightarrow \mu^+\mu^-$ (Figure 8b)

(3) $c\bar{c}$ bound state $J/\psi \rightarrow \mu^+\mu^-$ (Figure 8c, 8d)

7 Search for SUSY Particles

Searches in CDF for SUSY particles have been presented in detail [13,14]. Due to limitation in space in this write-up, we simply present an update on the results.

The missing transverse energy distribution is shown in Figure 9 for the 98 events with $\not\!\!E_T >$ 40 GeV and with 2 or more jets in the data corresponding to 4.4 pb^{-1} . We have studied background contributitions from : $W \rightarrow e+\nu$, $W \rightarrow \mu+\nu$, $W \rightarrow \tau+\nu$, $Z \rightarrow \nu\bar{\nu}$, QCD events for which the major background are the production and decay of heavy quarks. We estimated from our own data to have 86.4 $\pm$ 14.1(stat) $\pm$ 11.6(sys) background events from intermediate Boson decay, and 4 $\pm$ 4 events from QCD. For events with $\not\!\!E_T >$ 100 GeV, we expect 1.3 events from background and we observe 3 events in the data. For events with 4 jets, we expect 1.3 events from background and we observe 2 events. In a Monte Carlo study, we generated SUSY particles using ISAJET [11] together with a detector simulation, to obtain the number of events expected for various squark and gluino mass combinations.

From a search for SUSY particles in our missing E_T data, no excess of events were observed over the Standard Model background. The 90% CL limits on squark and gluino masses are shown in Figure 10.

8 Summary and Future Prospects

We have enjoyed searches for the top quark in the '88 – '89 run data and have advanced our experience with the analyses. The 95% CL lower limit for the mass of the top quark is 84 GeV/c^2 from a search for $e\mu$, ee, $\mu\mu$ central high P_T di-lepton events. The low P_T muon *b-tagging* search adds 30% of the $t\bar{t}$ detection efficiency and extends the lower limit on M_{top} to 89 GeV/c^2. We are working on extending the electron analysis to larger pseudo-rapidity in the smaller angle region.

In the next run, we plan to have a few times more integrated luminosity, and the analyses will be more efficient for searching for higher mass top quark. There will also be detector upgrades such as larger muon chamber coverage, and the Silicon Vertex Detector to tag the b quarks in the events. We expect to find the top in the '91 – '92 run with the planned luminosity of 25 pb^{-1} if the top mass is below 150 GeV/c^2. For the following run, we hope to have major upgrades for both the accelerator and CDF. With a goal of more than 100 pb^{-1}, we hope to cover the full M_{top} range allowed by the Standard Model. Meanwhile, we are also enjoying very nice b-quark and c-quark physics, and seeking SUSY.

References

[1] F. Abe *et al.*, Nucl. Instrum. Methods A271, 387 (1988).

[2] F. Abe *et al.*, Phys. Rev. Lett. 64, 147 (1990).

[3] F. Abe *et al.*, Phys. Rev. Lett. 64, 142 (1990).

[4] F. Abe *et al.*, Phys. Rev. Lett. 63, 720 (1989).

[5] F. Abe *et al.*, Phys. Rev. Lett. 64, 152 (1990).

[6] M. Dell'Orso, K. Kondo, H. Grassmann, A. Yagil, in these Proceedings.

[7] G. P. Yeh, Conference on the 4th Family of Quarks and Leptons, New York Academy of Sciences, Santa Monica, 1989. M. Shochet, Les Rencontres de Physique de la Valle d'Aoste, M. Greco Editor, Editions Frontieres, Gif-sur Yvette 1989, p195.

[8] P. Nason, S. Dawson and R.K. Ellis, Nucl. Phys. B303, 607 (1988).

[9] G. Altarelli, M. Diemoz, G. Martinelli and P. Nason, Nucl. Phys. B308, 724 (1988).

[10] For discussions on $M_T^{e\nu}$, see H. Baer, V. Barger, and R. J. N. Phillips, Phys. Lett.
B221, 398(1989) and J. Rosner, Phys. Rev. D39, 3297 (1989) ; D40, 1701 (1989).

[11] F. Paige and S. D. Protopopescu, BNL 38034 (1986).

[12] H. E. Haber and G. L. Kane, Phys. Rep. 117 , 75 (1985); S. Dawson, E. Eichten and
C. Quigg, Phys. Rev. D31, 1581 (1985).

[13] J. Freeman, Les Rencontres de Physique de la Valle d'Aoste, M. Greco Editor, Editions Frontieres, Gif-sur Yvette 1989, p297.

[14] CDF Collaboration, F. Abe et al., Phys. Rev. Lett. 64, 1825 (1989).

9 List of Figures

Figure 1: top quark production cross-section [8,9]

In each of Figures 2 to 6, there are 4 plots for the $t\bar{t}(M_{top} = 80)$, $t\bar{t}(M_{top} = 90)$, Z Monte Carlo samples and for the data. For the histograms, the plots for the $t\bar{t}$ samples have been normalized to 4.4 pb^{-1}, from the generated samples of 268 pb^{-1} and 732 pb^{-1}.

Figure 2: The distribution of the ee invariant mass, M_{ee}

Figure 3: The missing transverse energy distribution for ee events

Figure 4: The $\Delta\phi_{ee}$ distribution

Figure 5: $\Delta\phi_{ee}$ vs. missing E_T after the M_{ee} window cut

Figure 6: $\Delta\phi_{\mu\mu}$ vs. missing E_T after the $M_{\mu\mu}$ mass window cut

Figure 7: The 95% CL upper limit on the $t\bar{t}$ production cross section as a function of top quark mass. The parallel band is from the theoretical calculation of the $t\bar{t}$ production cross-section [8,9].

Figure 8: 8a: $B \rightarrow e + D^0 + X$; $D^0 \rightarrow K\pi$, 8b: $\Upsilon \rightarrow \mu^+\mu^-$, 8c: $J/\psi \rightarrow \mu^+\mu^-$, 8d: $J/\psi(2S) \rightarrow \mu^+\mu^-$. The invariant mass distributions are plotted for the opposite sign and same sign di-muons in 8b, 8c, and 8d.

Figure 9: missing E_T distribution for events with missing $E_T > 40$ GeV and with two or more jets

Figure 10: The 90% CL limits on squark and gluino masses

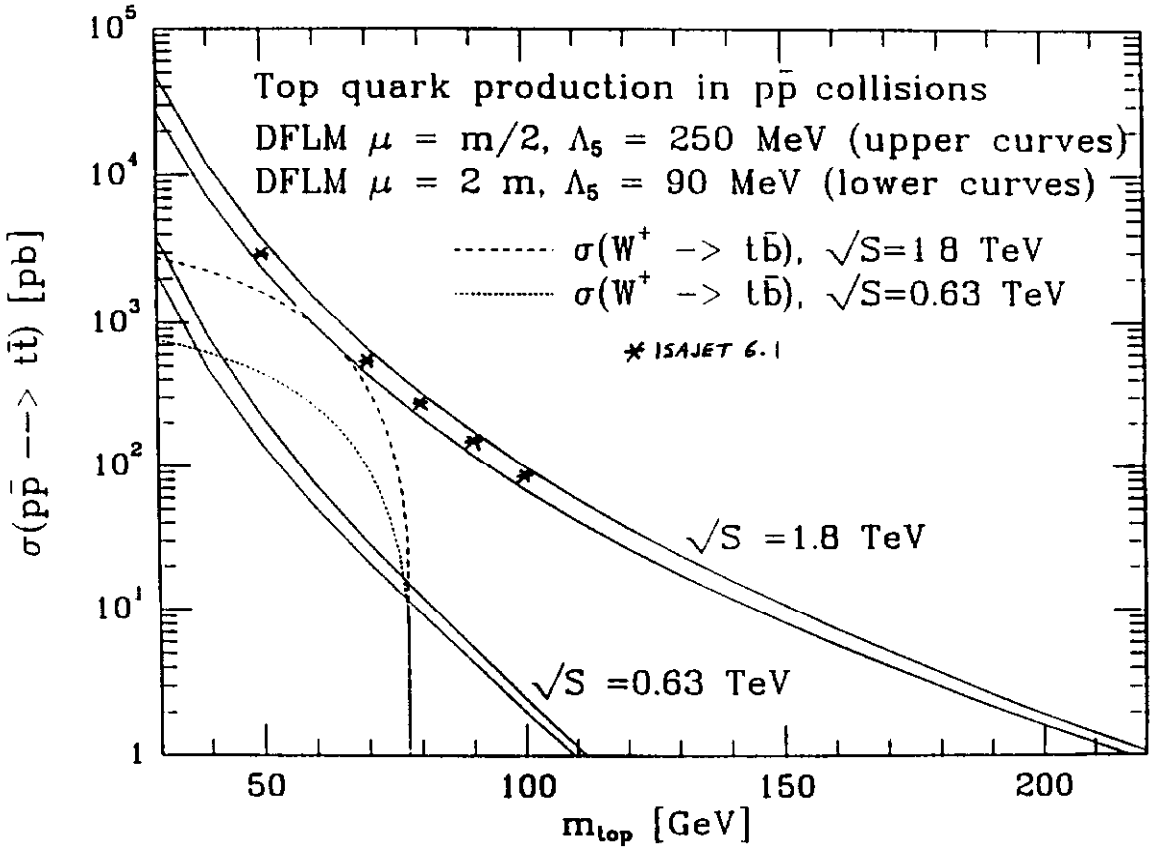

Figure 1: top quark production cross-section from references [8,9]

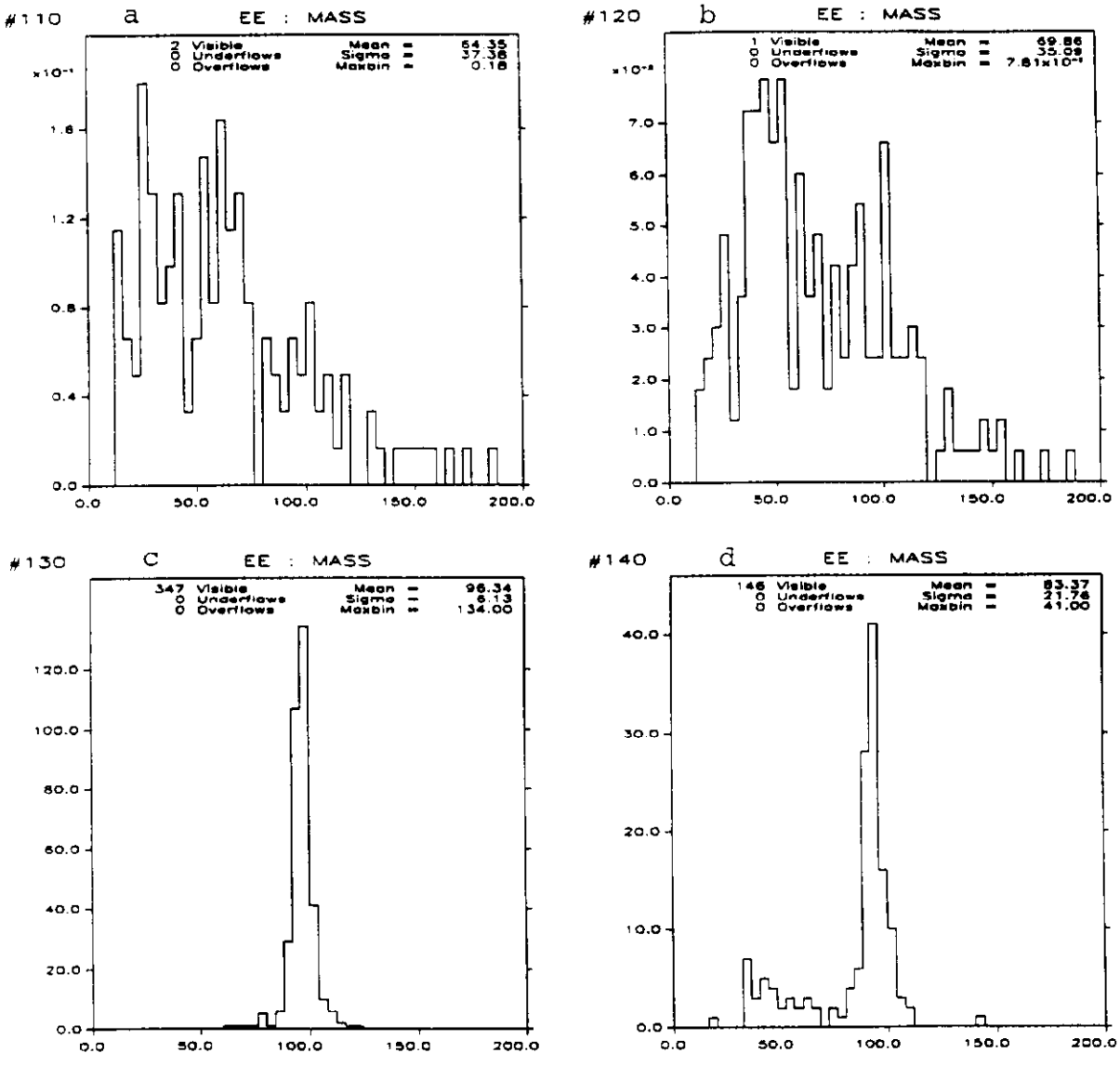

Figure 2: The distribution of the ee invariant mass, M_{ee}

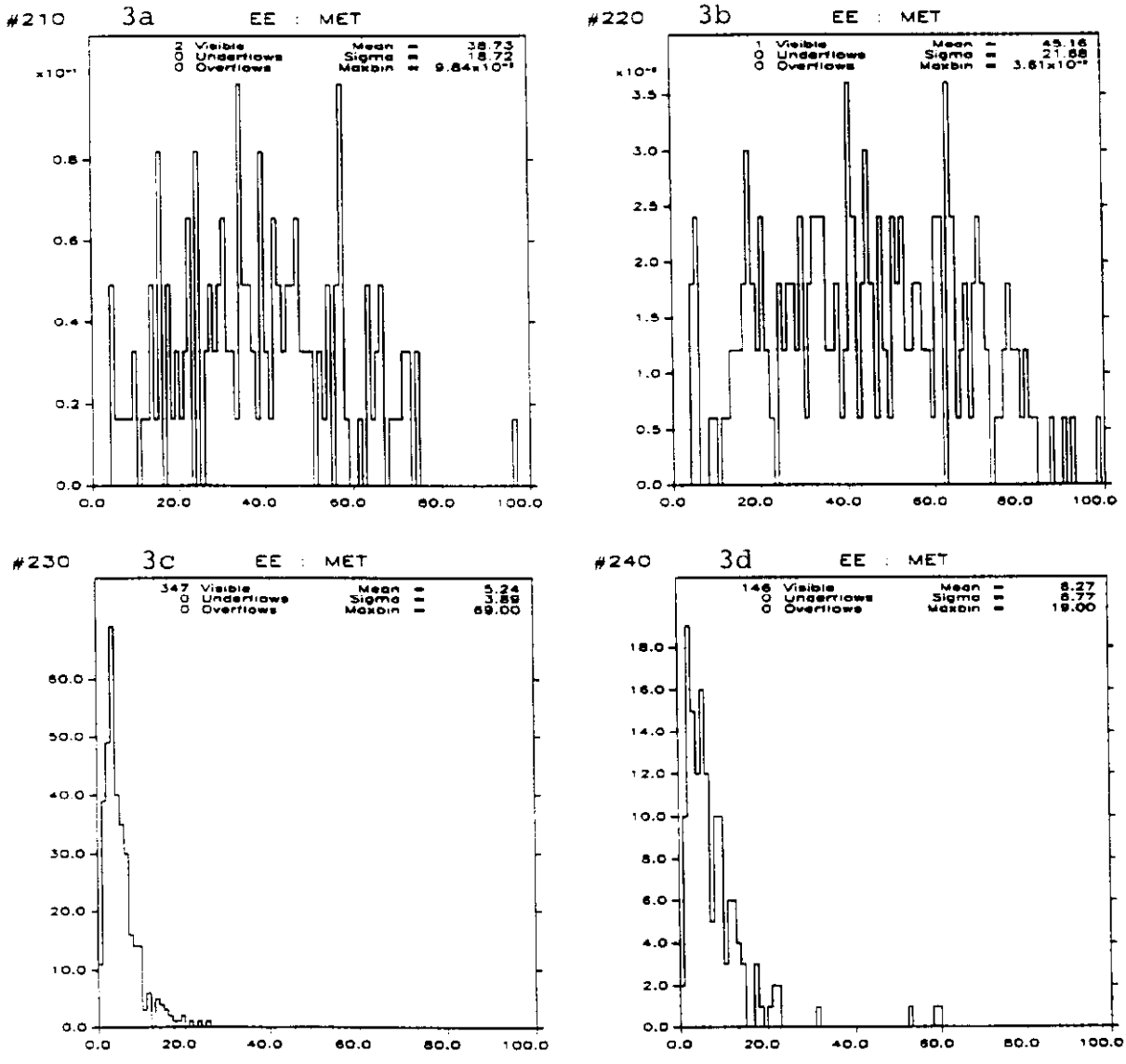

Figure 3: The missing transverse energy distribution for ee events

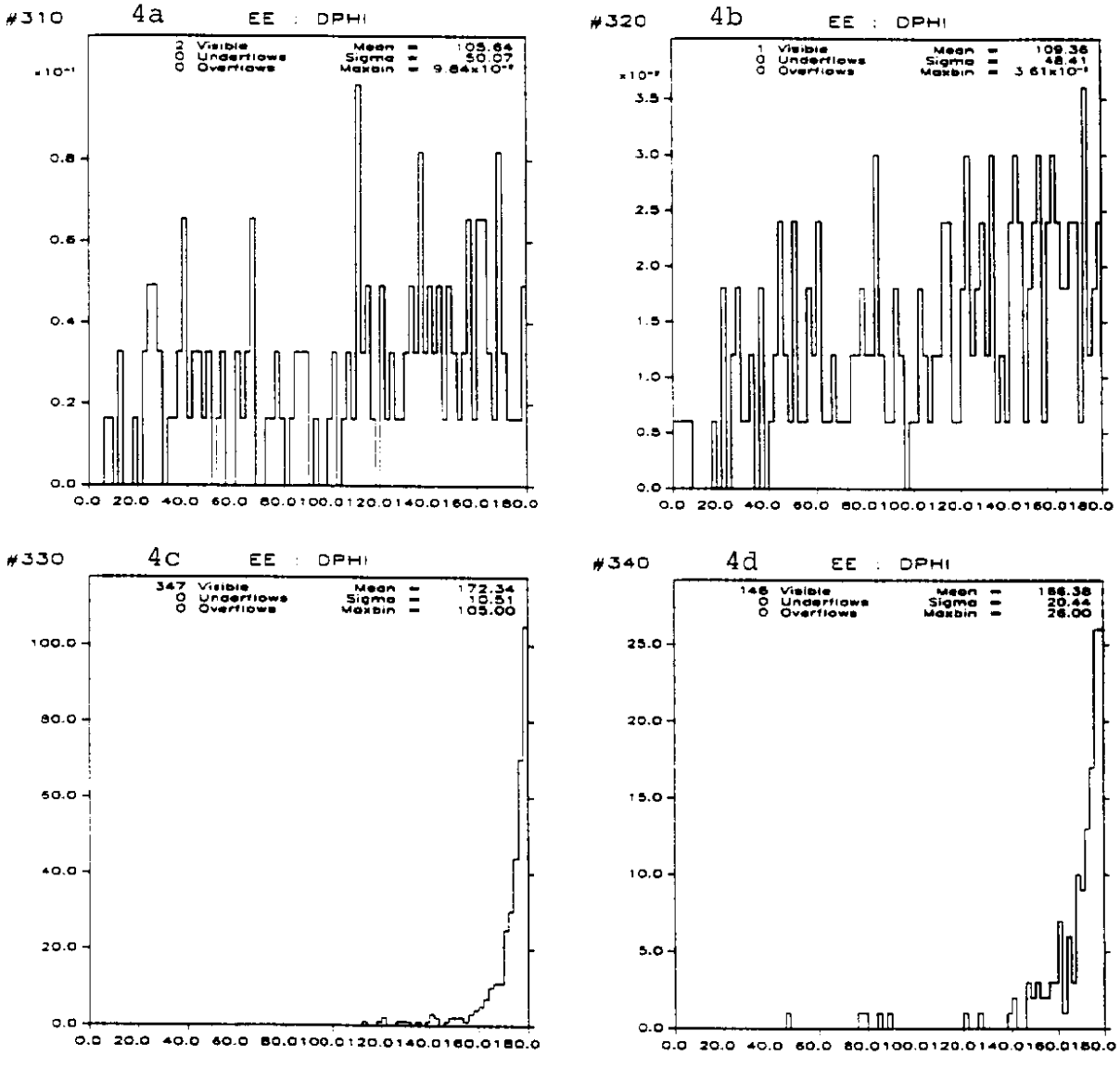

Figure 4: The $\Delta\phi_{ee}$ distribution

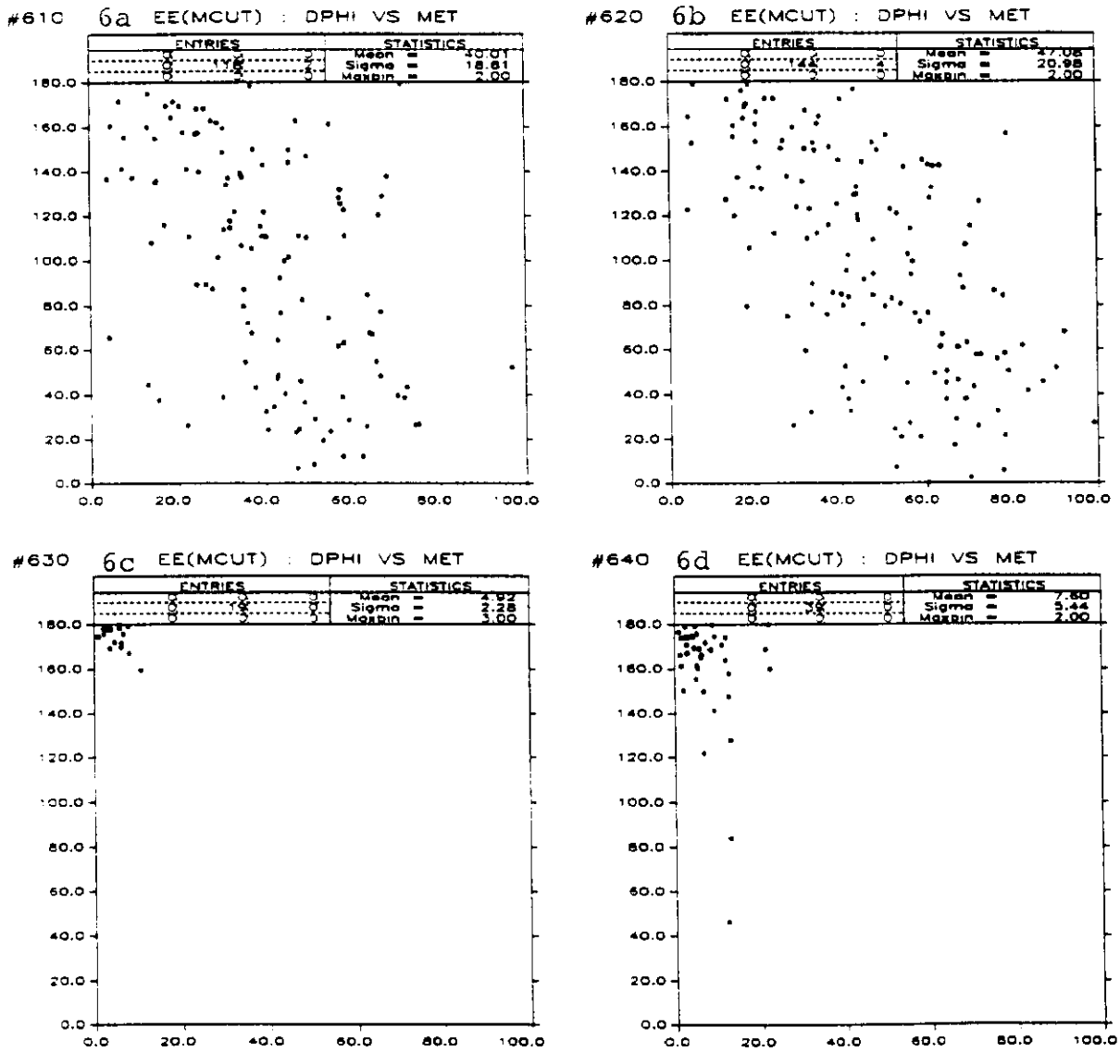

Figure 5: $\Delta\phi_{ee}$ vs. missing E_T after the M_{ee} window cut.

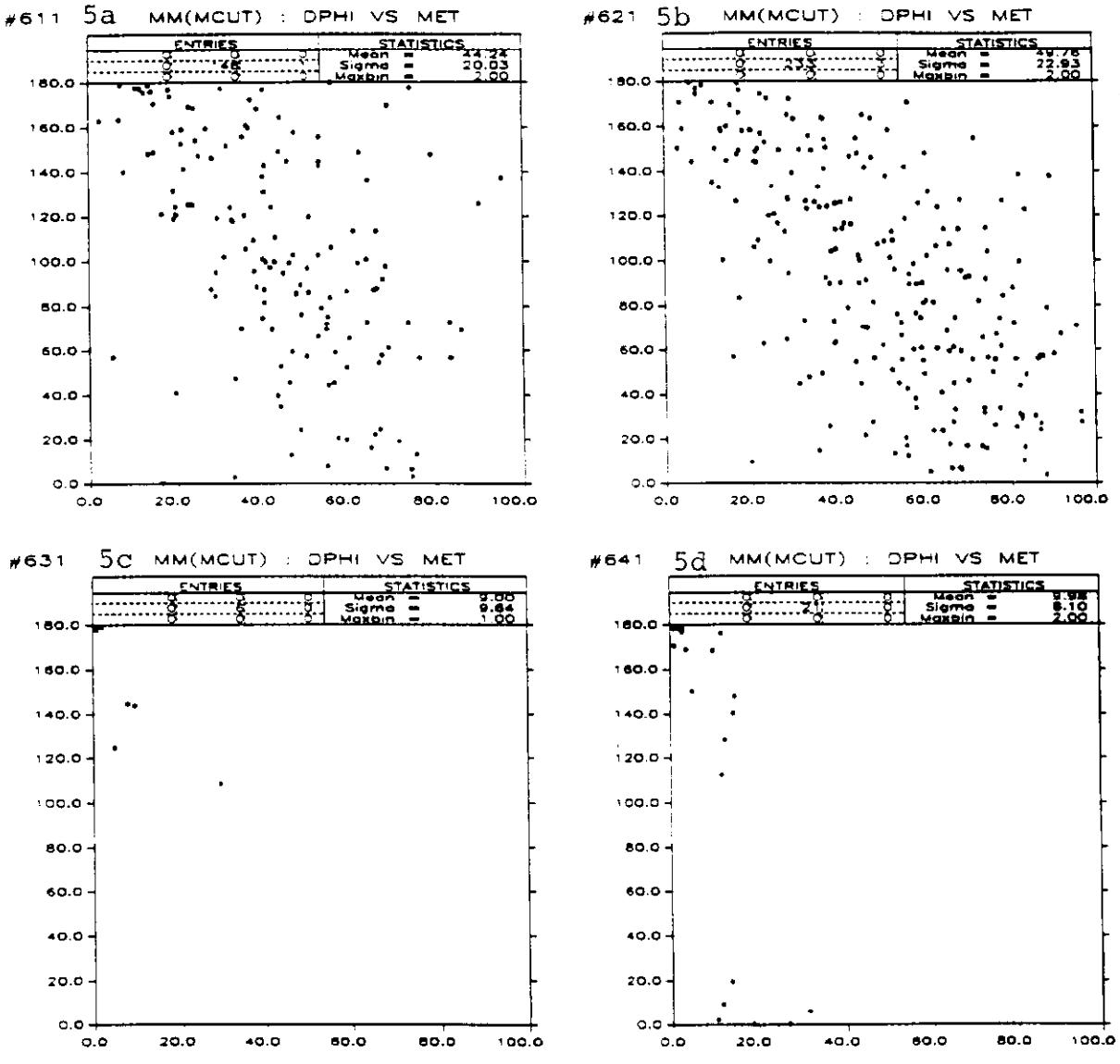

Figure 6: $\Delta\phi_{\mu\mu}$ vs. missing E_T after the $M_{\mu\mu}$ mass window cut.

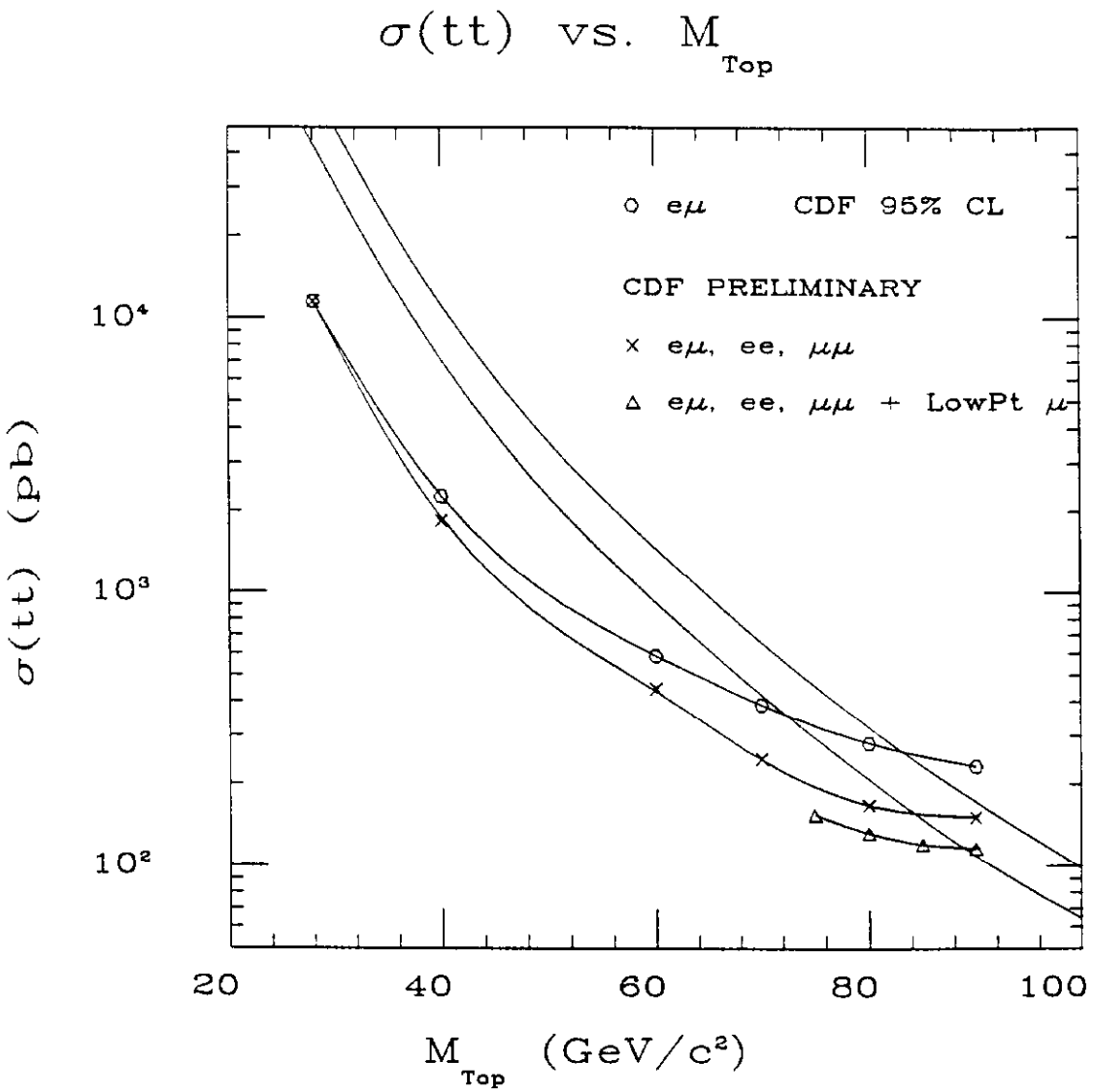

Figure 7: The 95% CL upper limit on the $t\bar{t}$ production cross section as a function of top quark mass. The parallel band is from the theoretical calculation of the $t\bar{t}$ production cross section [8,9].

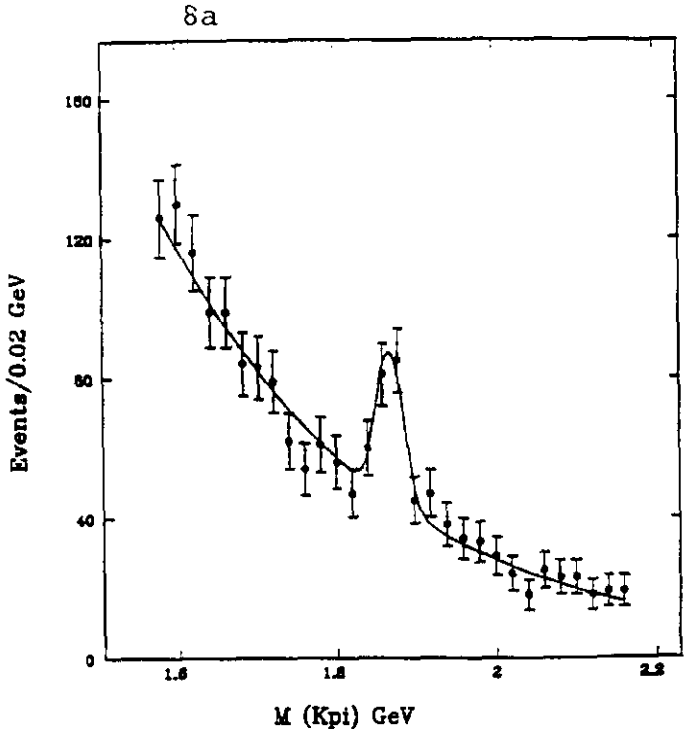

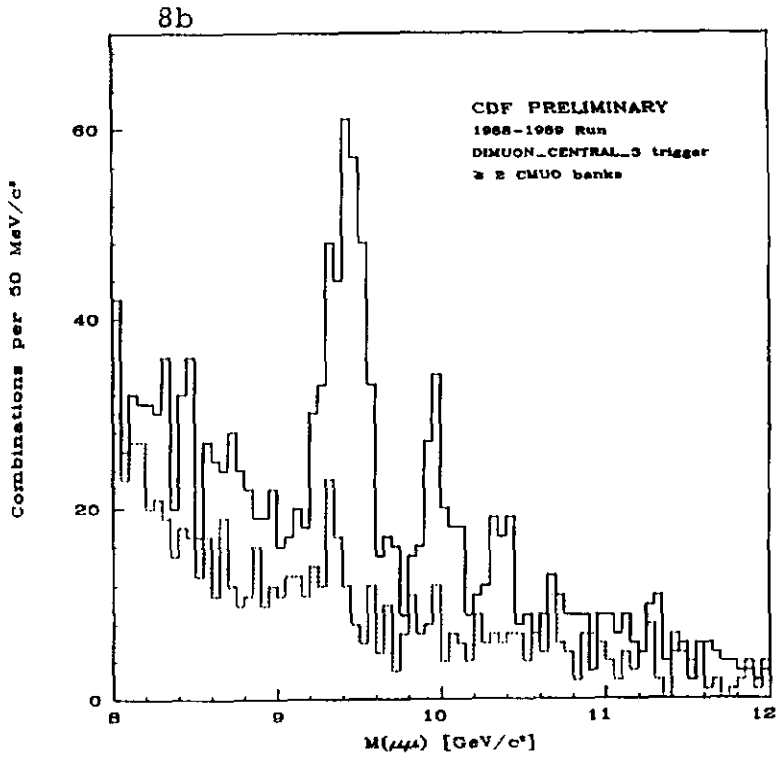

Figure 8: 8a: $B \rightarrow e + D^0 + X$; $D^0 \rightarrow K\pi$, 8b: $\Upsilon \rightarrow \mu^+\mu^-$

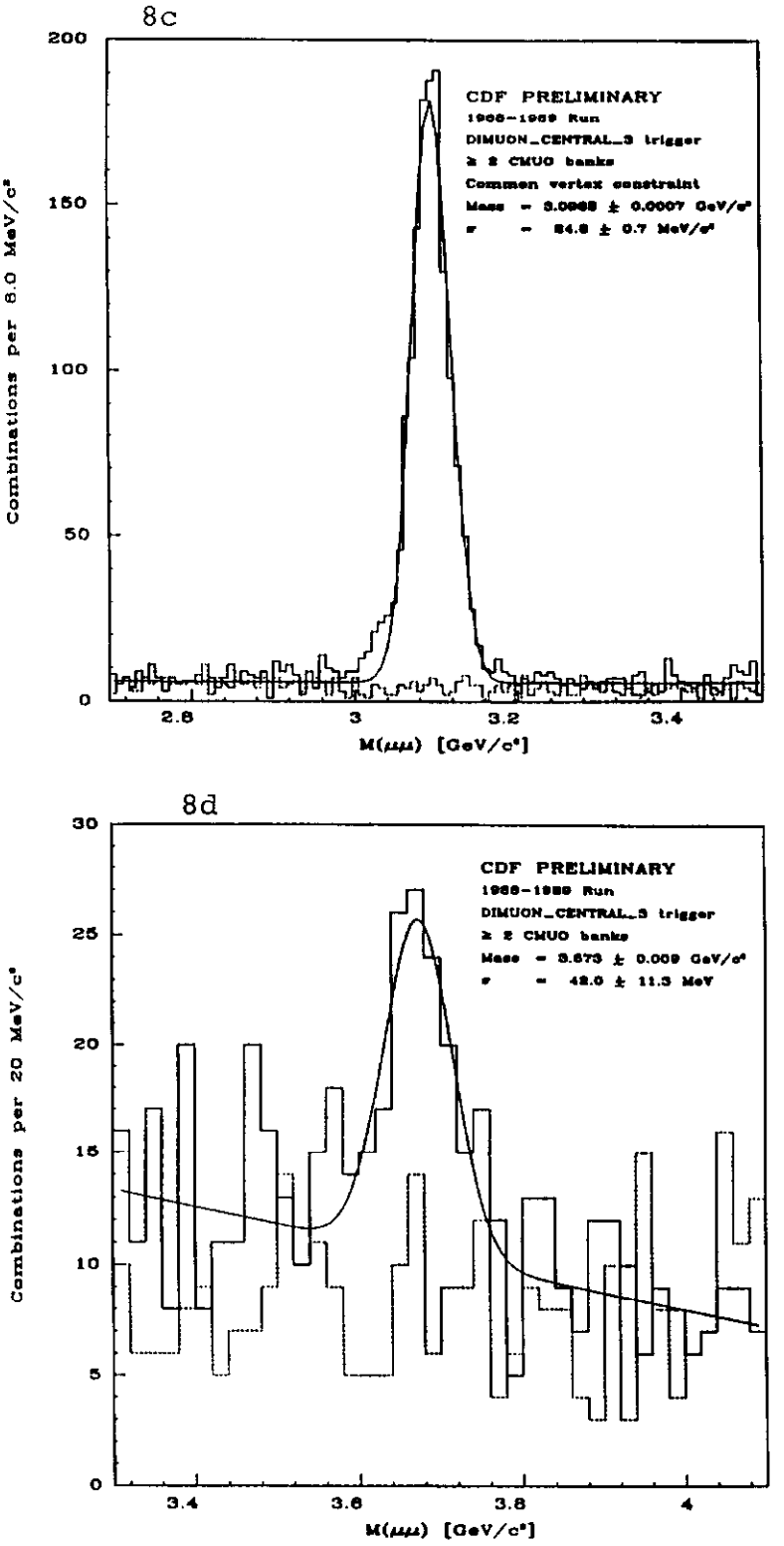

Figure 8: 8c: $J/\psi \rightarrow \mu^+\mu^-$, 8d: $J/\psi(2S) \rightarrow \mu^+\mu^-$

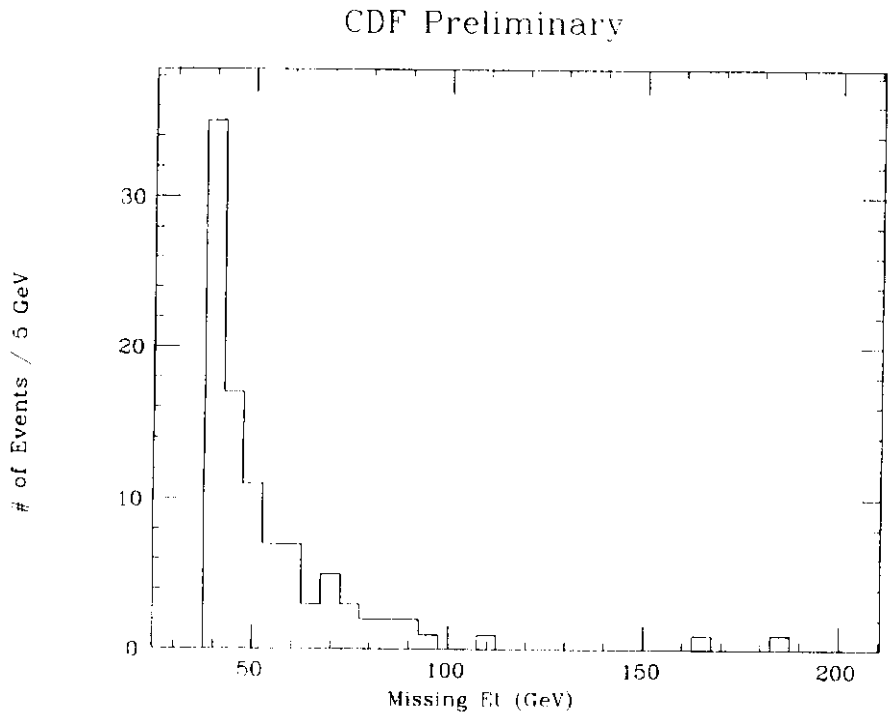

Figure 9: missing E_T distribution for events with missing E_T > 40 GeV and with two or more jets

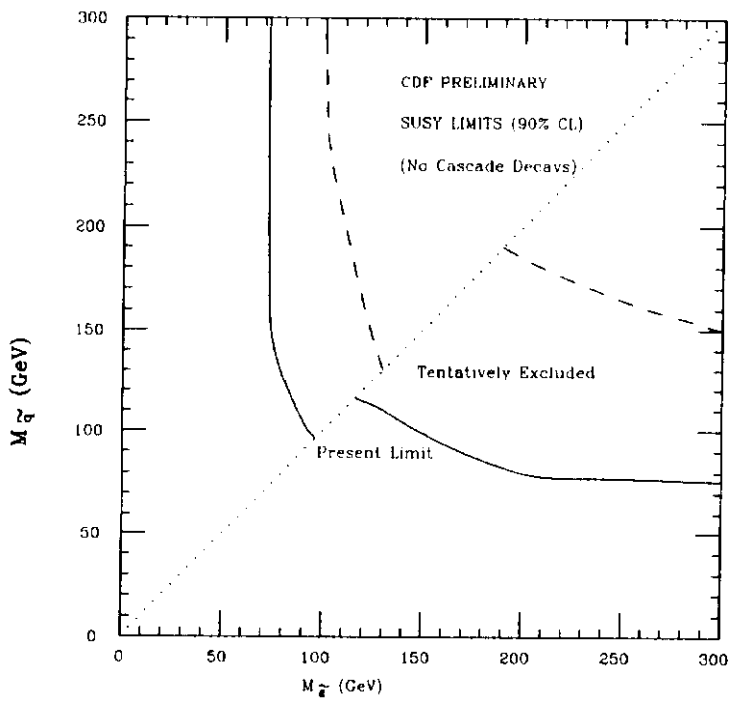

Figure 10: The 90% CL limits on squark and gluino masses